



# Degradation of Microcystin-LR in water: Hydrolysis of peptide bonds catalyzed by maghemite under visible light



Yanfen Fang<sup>a,b</sup>, Yu Zhang<sup>b</sup>, Wanhong Ma<sup>a,\*</sup>, David M. Johnson<sup>a,b</sup>, Ying-ping Huang<sup>a,b,\*</sup>

<sup>a</sup> Innovation Center for Geo-Hazards and Eco-Environment in Three Gorges Area, Yichang 443002, Hubei Province, China

<sup>b</sup> Engineering Research Center of Eco-environment in Three Gorges Reservoir Region, Ministry of Education, China Three Gorges University, Yichang 443002, China

## ARTICLE INFO

### Article history:

Received 2 February 2014

Received in revised form 27 April 2014

Accepted 11 May 2014

Available online 4 June 2014

### Keywords:

Maghemite

Microcystin-LR

Hydrolysis

Peptide bonds

## ABSTRACT

Maghemite, an abundant iron-oxide mineral, was investigated as a visible light catalyst for decomposing and mineralizing Microcystin-LR (MC-LR) in water using hydrogen peroxide ( $H_2O_2$ ) as the initial oxidant. Interestingly, of the twelve intermediates identified by LC-MS, half were products of MC-LR peptide bond hydrolysis rather than the oxidation products typical of photocatalytic oxidation (PCO). The catalytic hydrolysis of MC-LR by maghemite and visible light has not been previously reported. Detailed examination of intermediates provided insight into the catalytic pathway. Electron spin resonance (ESR) spectra revealed that visible light irradiation does not increase hydroxyl radical ( $\bullet OH$ ) production from  $H_2O_2$  decomposition. Visible light appears to play a new role in this unique PCO system, generating Brønsted sites on the maghemite surface via a metal ligand charge transfer (MLCT), rather than producing  $\bullet OH$  from  $H_2O_2$ . Because opening the cyclic peptide structure detoxifies MC-LR, this catalytic system could be uniquely efficient in detoxifying MC-LR in the presence of relatively high levels of natural organic matter (NOM). This work introduces a new means of selectively and effectively detoxifying MCs in water using an inexpensive, environmentally friendly and bio-compatible mineral.

© 2014 Elsevier B.V. All rights reserved.

## 1. Introduction

Microcystins (MCs) are cyclic peptides released by cyanobacteria during algal blooms in eutrophic waters and among the most common of the cyanotoxins [1,2]. The cyclic peptide structure, shared across MCs, was first characterized in 1986 [3]. MCs inhibit phosphatase PP1 and PP2A, produce lesions in the liver and promote cancer [4–7]. Microcystin-LR (MC-LR, Fig. 1) is one of the most toxic and widely distributed MCs in natural waters and has been used as a model contaminant for MCs in numerous investigations [8]. Health-related cases in humans and animals caused by MC-LR were little reported until a fatal human incident occurred in 1996 [9]. The World Health Organization (WHO) has set the provisional concentration limit of MC-LR for potable water at  $1 \mu g/L$  [10].

The stability of the cyclic peptide structure prevents effective removal of MC-LR by conventional water or wastewater treatment.

Among the advanced oxidation technologies (AOTs), photocatalytic oxidation (PCO) is the most promising treatment technology [11,12]. For example, both  $TiO_2$  photocatalysis [11,13,14] and the UV-Fenton system [15] effectively degrade MCs in water by generating highly reactive hydroxyl radicals ( $\bullet OH$ ). Recently, a range of heterogeneous catalysts, including various iron and manganese oxides, have been used to degrade refractory organic compounds by activating  $H_2O_2$  to produce  $\bullet OH$  [16,17]. However, most PCO processes require UV irradiation, severely restricting PCO application for environmental remediation because sunlight contains only 4–5% UV. Some iron-bearing mineral oxides are activated by visible light due to metal ligand charge transfer (MLCT) on the surface [18], but the  $\bullet OH$  yield depends on surface  $Fe(III)/Fe(II)$  catalytic recycling and is typically low [19]. To date, iron-bearing minerals have rarely used visible light to enhance degradation of organic pollutants such as MC-LR [20]. Furthermore, trace water pollutants such as MCs are particularly difficult to remove by  $\bullet OH$  oxidation alone because  $\bullet OH$  is not selective and other natural organic matter (NOM) is typically present at much higher concentrations than target pollutants. Finding an iron oxide mineral, activated by visible light, that effectively detoxifies MCs in the presence of NOM remains an important, but unmet, challenge.

\* Corresponding author at: Innovation Center for Geo-Hazards and Eco-Environment in Three Gorges Area, Yichang 443002, Hubei Province, China. Tel.: +86 717 6397488; fax: +86 717 6395966.

E-mail addresses: [huangyp@ctgu.edu.cn](mailto:huangyp@ctgu.edu.cn), [chem.ctgu@126.com](mailto:chem.ctgu@126.com), [yingpinghuang@126.com](mailto:yingpinghuang@126.com) (Y.-p. Huang).

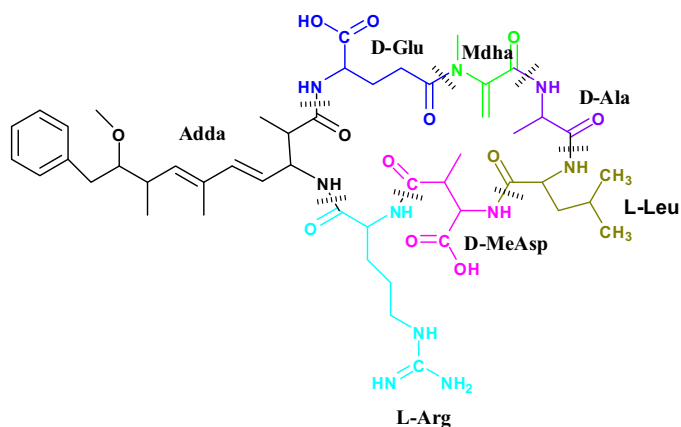


**Fig. 1.** The structure of Microcystin-LR (MC-LR). Adda is (2*s*,3*s*,8*s*,9*s*)-3-amino-9-methoxy-2,6,8-trimethyl-10-phenyldeca-4(*E*),6(*E*)-dienoic acid; D-Glu is D-glutamic acid; Mdha is N-methyl-dehydroalanine; D-Ala is D-alanine; L-Leu is L-Leucine; D-Me-Asp is D-erythro- $\beta$ -methaspartic acid; L-Arg is L-arginine.

In the search for a selective and effective means of degrading MC-LR, hydrolysis of the cyclic peptide bonds could be a breakthrough in visible light assisted PCO. Selectivity is inherently high because multiple peptide bonds are rare in most NOM and organic pollutants. Detoxification is effective because catalytic hydrolysis of a peptide bond opens the stable macrocyclic structure of MC-LR, altering the binding site and significantly decreasing inhibition of the phosphatase, PPA1 [4]. Dionysiou and co-workers [11] indicated that complete MC-LR transformation by TiO<sub>2</sub>/UV photocatalysis still leaves significant toxicity (PPA1 inhibition remains at nearly 100%). Catalytic conversion of MC-LR by TiO<sub>2</sub> leads to hydroxylation of the Adda double bonds and does not prevent binding of the Mdha moiety of MC-LR to PPA1. In contrast, when a small amount of H<sub>2</sub>O<sub>2</sub> was added to this TiO<sub>2</sub>/UV system, PPA1 inhibition by MC-LR degradation products rapidly approached zero [11]. This could be attributed to oxidative hydrolysis of MC-LR peptide bonds mediated by Brønsted sites generated by H<sub>2</sub>O<sub>2</sub> on the surface of the TiO<sub>2</sub> catalyst. It has been demonstrated previously that ring opening of cyclic peptide bonds of Microcystin-LR by bacterial microcystinase effectively renders the compound nontoxic by reducing the interaction with the target protein phosphatase [21]. Recently, N-protected and free Adda amino residues from the hydrolysis of Microcystin-LR was proved nontoxicity [22]. Compared with mineralization, detoxification of MCs by photocatalytic hydrolysis of peptide bonds obviously requires small quantities of H<sub>2</sub>O<sub>2</sub>, making MC treatment in water more economic.

Hydrolysis of peptide bonds can be catalyzed by Brønsted acids and bases and metal complexes. Glycylglycine, for example, is hydrolyzed with a half-life of approximately 2 days in 1 M NaOH and 150 days in 1 M HCl at 25 °C, but with a half-life of several years under neutral pH conditions [23,24]. Peptide bonds are rapidly cleaved by complexes of copper, molybdenum and zirconium [25–27], but metal complexes are expensive and some produce harmful environmental effects. Recently, peptide bond hydrolysis at the water–pyrite interface under extreme thermodynamic conditions has been reported [28,29] and the results are relevant to biogeochemistry and environmental chemistry. Maghemite, for example, has great potential for decontaminating soils, sediments, and water [30]. However, production of Brønsted sites on the surface of maghemite in a PCO system that catalyze hydrolysis of MC peptides has not been reported.

In the work reported here, maghemite was used as a visible light catalyst to degrade MC-LR in water at neutral pH using H<sub>2</sub>O<sub>2</sub> as the initial oxidant. Hydrolytic cleavage of the stable ring structure facilitates oxidative decomposition. The

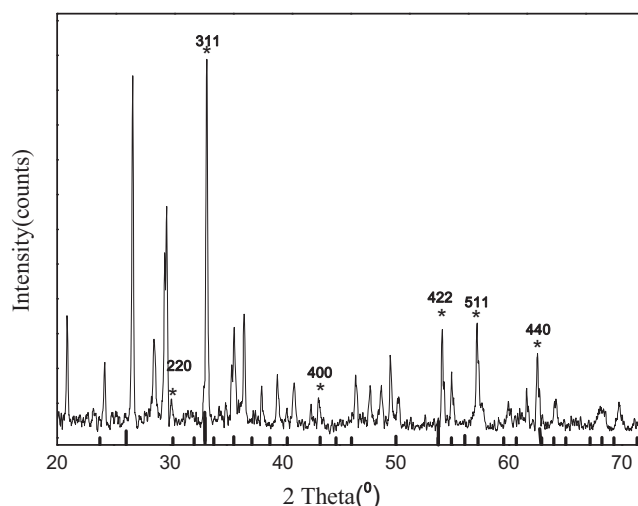


**Fig. 2.** XRD pattern of maghemite. Note: the positions and intensities of the diffraction lines of  $\gamma$ -Fe<sub>2</sub>O<sub>3</sub> (JCPDS file 39-1346) are indicated by tic marks just above the horizontal axis.

unique degradation products of MC-LR were identified using liquid chromatography-mass spectroscopy (LC-MS) and  $\cdot$ OH formation was monitored using electron spin resonance (ESR). Our results are quite different from previously investigated PCO systems: (1) catalytic hydrolysis reactions are important to the degradation of MC-LR by the maghemite photocatalyst and (2) visible light irradiation does not increase production of  $\cdot$ OH from H<sub>2</sub>O<sub>2</sub> decomposition but increases H<sub>2</sub>O<sub>2</sub> utilization efficiency to 100% for MC-LR degradation. The maghemite PCO system reported here introduces a promising new approach for selectively and effectively detoxifying MCs in treatment of water with high levels of NOM.

## 2. Materials and methods

### 2.1. Reagents

Maghemite samples were provided by the Central-South Research Institute of Metallurgical Geology (Hubei, China). The maghemite was washed (1.6 m<sup>3</sup> water/t mineral) to remove natural contaminants, ground and sieved (100-mesh) to obtain crystal particles  $\leq 150 \mu\text{m}$ . The maghemite was characterized using X-ray diffraction (XRD) (Bruker D8 Advance II, Germany) with a CuK  $\alpha$  radiation source and a scan rate of 2.4°/min from 20° to 80°. Results indicate the typical hexagonal structure of maghemite with unit-cell parameters  $a = b = c = 8.351 \text{ \AA}$ . The characteristic peaks of the primary components (Fig. 2) are designated with asterisks (\*) and they compare well with the reference material ( $\gamma$ -Fe<sub>2</sub>O<sub>3</sub>, JCPDS 39-1346). The specific surface area was 1.68 m<sup>2</sup>/g as determined by BET surface area analysis (Micromeritics ASAP 2020, USA).

MC-LR (95%; FW 995.2 g/mol) was purchased from Express Technology Co., Ltd (China). A 50 mg/L MC-LR standard solution was obtained by dissolving 0.25 mg MC-LR in 5 mL of methanol (HPLC grade). The standard was stored at  $-20^\circ\text{C}$  and 5.0 mL test solutions containing 2.0 mg/L MC-LR were prepared by mixing 0.2 mL MC-LR standard solution with 4.80 mL of water (autoclaved by Milli-Q® Synthesis A10, Millipore Corp., Billerica, MA, USA). Standard Fulvic acid sample (adjusted by Nordic lake fulvic acid obtained from, 1R105F) was purchased from International Humic Substance Society (HISS). All reagents were analytical grade and used without further purification.

**Table 1**  
LC-MS retention time, mass to charge ratio ( $m/z$ ) and relative peak area (count  $\times 10^5$ ) after specified irradiation times for intermediate products formed during degradation of MC-LR.

Retention time (min)	Products	$t$ (h)	$a$	$b$	$c_1, c_2$	$d$	$e_1$	$e_2$	$e_3$	$f$	$g$	$h_1$	$h_2$	$i_1$	$i_2$	$j$	$k$	$l$	MC-LR
48.0–48.2			743 <sup>a</sup>	700 <sup>a</sup>	918 <sup>a</sup>	884 <sup>a</sup>	1029 <sup>a</sup>	1029 <sup>a</sup>	1029 <sup>a</sup>	851 <sup>a</sup>	759 <sup>a</sup>	829 <sup>a</sup>	829 <sup>a</sup>	1013 <sup>a</sup>	1013 <sup>a</sup>	0	0.057	783 <sup>a</sup>	995 <sup>a</sup>
48.0–48.2			4.75	1.74	1.06	0.52	0.072	0.065	0.035	0.091	0.24	0.28	0.22	0.20	0.20	0	0.019	0.019	18.27
2.0			5.76	2.47	1.10	0.83	0.31	0.22	0.059	0.31	0.25	0.20	0.23	0.23	0.10	0.085	0.036	0.02	11.68
3.5			6.2	2.92	1.15	0.86	0.5	0.31	0.063	0.35	0.37	0.21	0.20	0.18	0.042	0.14	0.038	0.036	9.72
5.0			5.23	2.06	1.19	0.82	0.66	0.37	0.064	0.43	0.18	0.22	0.19	0.15	0.12	0.13	0.057	0.017	7.36
6.5			4.65	2.30	1.20	0.63	0.79	0.47	0.046	0.18	0.16	0.16	0.15	0.091	0.06	0.10	0.063	0.014	5.01
8.0			3.89	2.10	1.00	0.54	0.53	0.38	0.012	0.14	0.076	0.14	0.12	0.082	0.033	0.05	0.064	0.01	1.67
10			3.70	2.20	0.88	0.53	0.095	0.014	0.005	0.08	0.10	0.12	0.08	0.027	0	0.002	0.04	0.05	0.51

<sup>a</sup>  $[M+H]^+(m/z)$ .

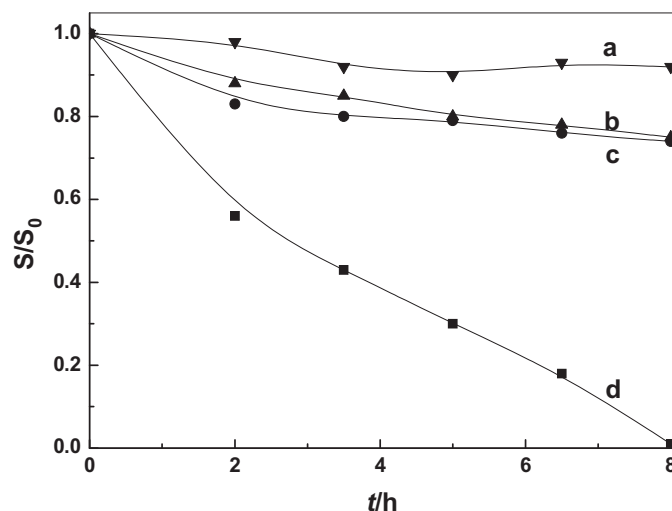


**Fig. 3.** MC-LR (2.0 mg/L) degradation curves at neutral pH in maghemite (240 mg/L) and  $H_2O_2$  ( $1 \times 10^{-4}$  mol/L) under the following conditions: 5 mL MC-LR solution (methanol/ $H_2O$ , v/v 0.2/4.8). (a) dark/maghemite/MC-LR; (b) vis/MC-LR/ $H_2O_2$ ; (c) dark/maghemite/MC-LR/ $H_2O_2$ ; (d) vis/maghemite/MC-LR/ $H_2O_2$ .

## 2.2. Photocatalytic process

Photocatalytic reactions were carried out in a PCO chamber (Xujiang Mechanical and Electrical Factory, Nanjing). The visible light source was a 250-W xenon lamp (Institute of Electric Light source, Beijing, China) positioned inside a cylindrical Pyrex reactor and surrounded by a circulating water jacket for cooling. To ensure illumination by visible light only, a cutoff filter was placed outside the Pyrex jacket to eliminate radiation with  $\lambda < 420$  nm. 10 mL of 2.0 mg/L MC-LR and 2.4 mg of maghemite powder was placed in the Pyrex reaction vessel. Prior to irradiation, the suspensions were magnetically stirred in the dark for 2 h to ensure adsorption/desorption equilibrium established. Hydrogen peroxide ( $H_2O_2$ ) was then added to the reaction vessel to give an initial concentration of  $1.0 \times 10^{-4}$  mol/L and the pH was adjusted to 7.0 using 1 M NaOH or HCl. At specified reaction times, 300  $\mu$ L samples of the reaction mixture were collected, centrifuged, and filtered using a membrane filter (Millipore, USA, 0.22  $\mu$ m) to remove

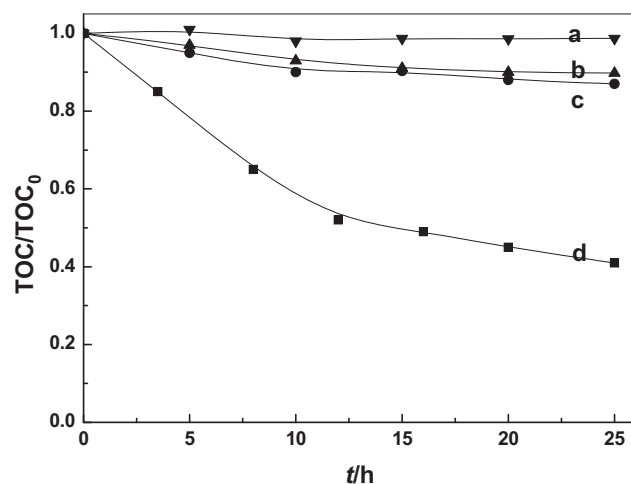


**Fig. 4.** Change in TOC during MC-LR (2.0 mg/L) degradation at neutral pH in maghemite (240 mg/L) and  $H_2O_2$  ( $1 \times 10^{-4}$  mol/L) under the following conditions: 5 mL MC-LR solution (methanol/ $H_2O$ , v/v 0.2/4.8). (a) dark/maghemite/MC-LR; (b) vis/MC-LR/ $H_2O_2$ ; (c) dark/maghemite/MC-LR/ $H_2O_2$ ; (d) vis/maghemite/MC-LR/ $H_2O_2$ .

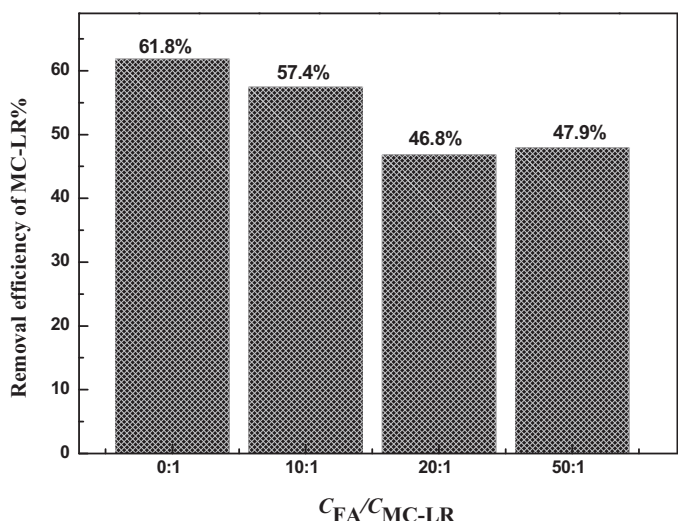


**Fig. 5.** Effect of FA on the removal efficiency of MC-LR. 240 mg/L maghemite,  $C_{H_2O_2} = 1 \times 10^{-4}$  mol/L,  $C_{MC-LR} = 2.0$  mg/L,  $C_{FA}/C_{MC-LR} = 0:1, 10:1, 20:1$  and  $50:1$ , neutral pH, irradiated by visible light for 4 h. Standard Fulvic acid sample (adjusted by Nordic lake fulvic acid obtained from 1R105F) was purchased from International Humic Substance Society (HISS).

catalyst particles. The filtrate was analyzed using the methods described below.

### 2.3. Analytical methods

MC-LR was determined using HPLC (Waters 600 HPLC, Waters 2998 photodiode-array detector, USA) with a Kromasil C18 column (4.6 mm  $\times$  150 mm, 10  $\mu$ m particle size). The mobile phase was water and methanol (65:35, v/v) containing 0.05% trifluoroacetic acid (TFA). The flow rate, injection volume, column temperature and detection wavelength were 0.8 mL/min, 20  $\mu$ L, 40  $^{\circ}$ C and 238 nm, respectively. Under these conditions, the elution time for MC-LR was  $\sim$ 8.9 min. Total organic carbon (TOC) was determined with a TOC analyzer (Jena N/C2100 TOC analyzer, Germany).

Hydroxyl radical levels were monitored by ESR (Bruker ESP 500E, Germany) with DMPO (5,5-dimethyl-1-pyrroline-N-oxide) spin trapping. The light source was a Quanta-Ray ND:YAG pulsed laser system ( $k=532$  nm, 10 Hz). The intensity at the center of the magnetic field, field sweep range, microwave frequency and power were 3486.70 G, 100.0 G, 100 kHz and 10.02 mW, respectively.

Reaction intermediates were monitored using LC/MS (Agilent G1315D DAD/amazon SL, USA) with full scanning ( $m/z$  300–1200) in the positive ion mode. Gradient elution was used with formic acid (pH=2.6) and acetonitrile as the mobile phase. Gradient elution was programmed as 0–20% acetonitrile (10 min) followed by an increase to 35% (10 min), 60% (15 min), and 80% (10 min).

Toxicity testing of MC-LR before and after the treatment: 19 male and 19 female Kunming mice (18–22 g, specific pathogen-free) were used for the study. All mice were housed in animal rooms. These mice were maintained on a 12 h light/dark cycle and had no restriction of eating or drinking. The research was performed in accordance to the “Guide for the Care and Use of Laboratory Animals” (China Three Gorges University). The untreated and treated (24 h degradation) MC-LR solutions (2 mg/L) were administered by gavage injection (i.g.) or intraperitoneal injection (i.p.) at a dose of 80  $\mu$ g/kg body weight after the animals had fasted for 18 h. The test animals were randomly divided into 4 groups, each group including an equal number of male and female mice; group A (control group, i.p., 8 mice), group B (untreated solution, i.g., 10 mice), group C (untreated solution, i.p., 10 mice) and group D (treated solution (24 h), i.p., 10 mice). Saline was injected into animals in the control group and all animals were released from fasting after being injected. The toxic response following i.g. injection is significantly less than the response produced by i.p. [31]. injection. All animals were observed daily throughout the 7 day test period.

## 3. Results and discussion

### 3.1. Photocatalytic degradation of MC-LR

The ability of maghemite to photocatalytically degrade MC-LR under different conditions is displayed in Fig. 3. Degradation of MC-LR without  $H_2O_2$  was negligible in the dark after 8 h (a), indicating that maghemite alone does not catalyze oxidative degradation or hydrolysis of MC-LR. Nearly 20% of MC-LR was decomposed under irradiation when  $H_2O_2$  was added without maghemite (b). In the dark, a small quantity of MC-LR was decomposed by the maghemite/ $H_2O_2$  system (c) with reaction rate constant  $k=0.04$  min $^{-1}$ , according to pseudo-first order kinetics. The maghemite catalyst activates  $H_2O_2$  and partially degrades MC-LR without light irradiation. When the system containing both maghemite and  $H_2O_2$  was irradiated with visible light, a very rapid degradation of MC-LR took place (d), with  $k=0.289$  min $^{-1}$ . It should be noted that there was methanol (4%, v/v) in the reaction solution and methanol efficiently scavenges  $\cdot OH$ . This reduces indiscriminate oxidative decomposition and allows the interaction between

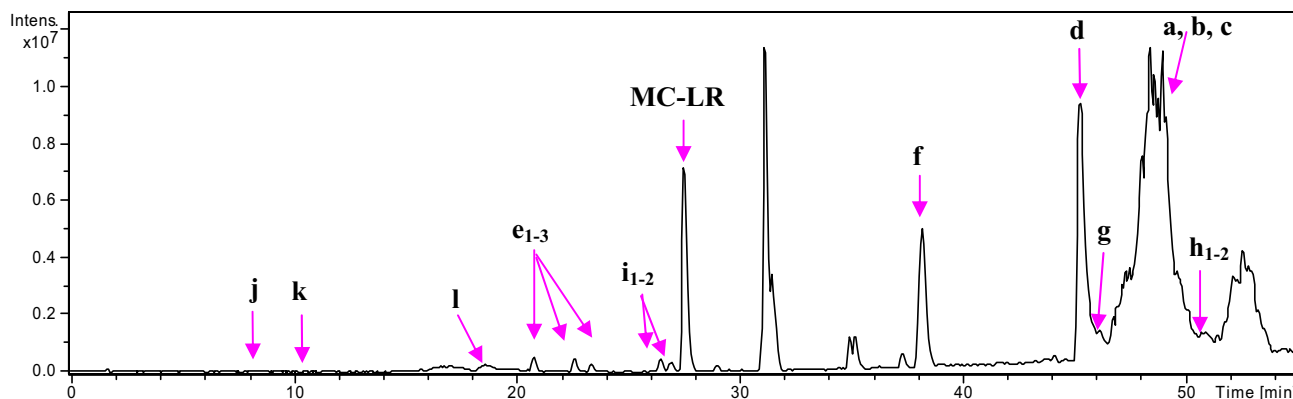


**Fig. 6.** Total ion chromatogram (TIC) obtained during MC-LR (2.0 mg/L) degradation at neutral pH in maghemite (240 mg/L) and  $H_2O_2$  ( $1 \times 10^{-4}$  mol/L) after 5 h of visible light irradiation.

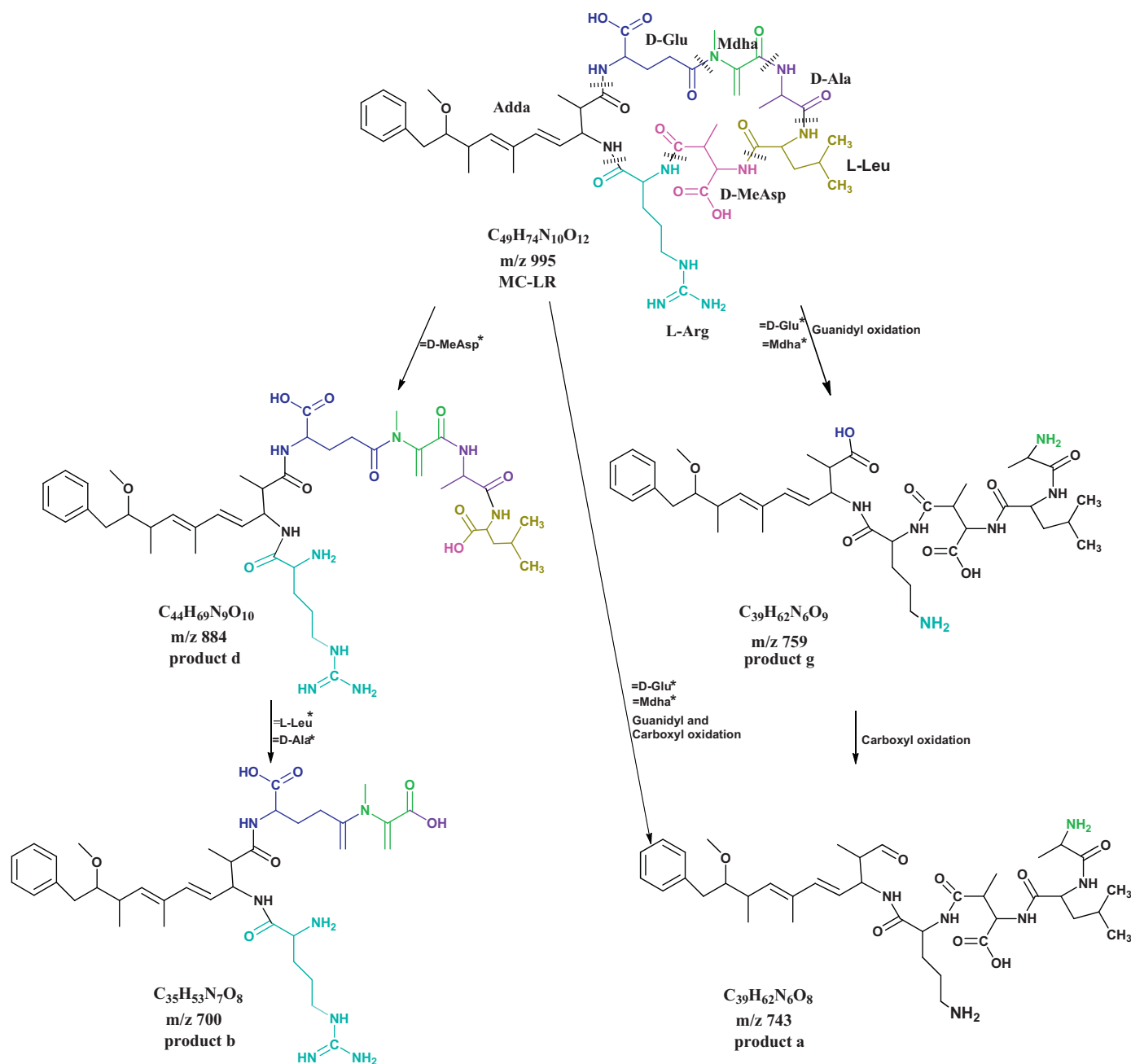


**Fig. 7.** Proposed reaction sequences for photocatalytic hydrolysis and partial oxidative hydrolysis of MC-LR. (a) Catalytic hydrolysis of MC-LR peptide bonds without Adda oxidation; (b) catalytic hydrolysis of MC-LR peptide bonds after hydroxylation of the Adda benzene ring.

visible light and maghemite to selectively degrade MC-LR by peptide bond hydrolysis.

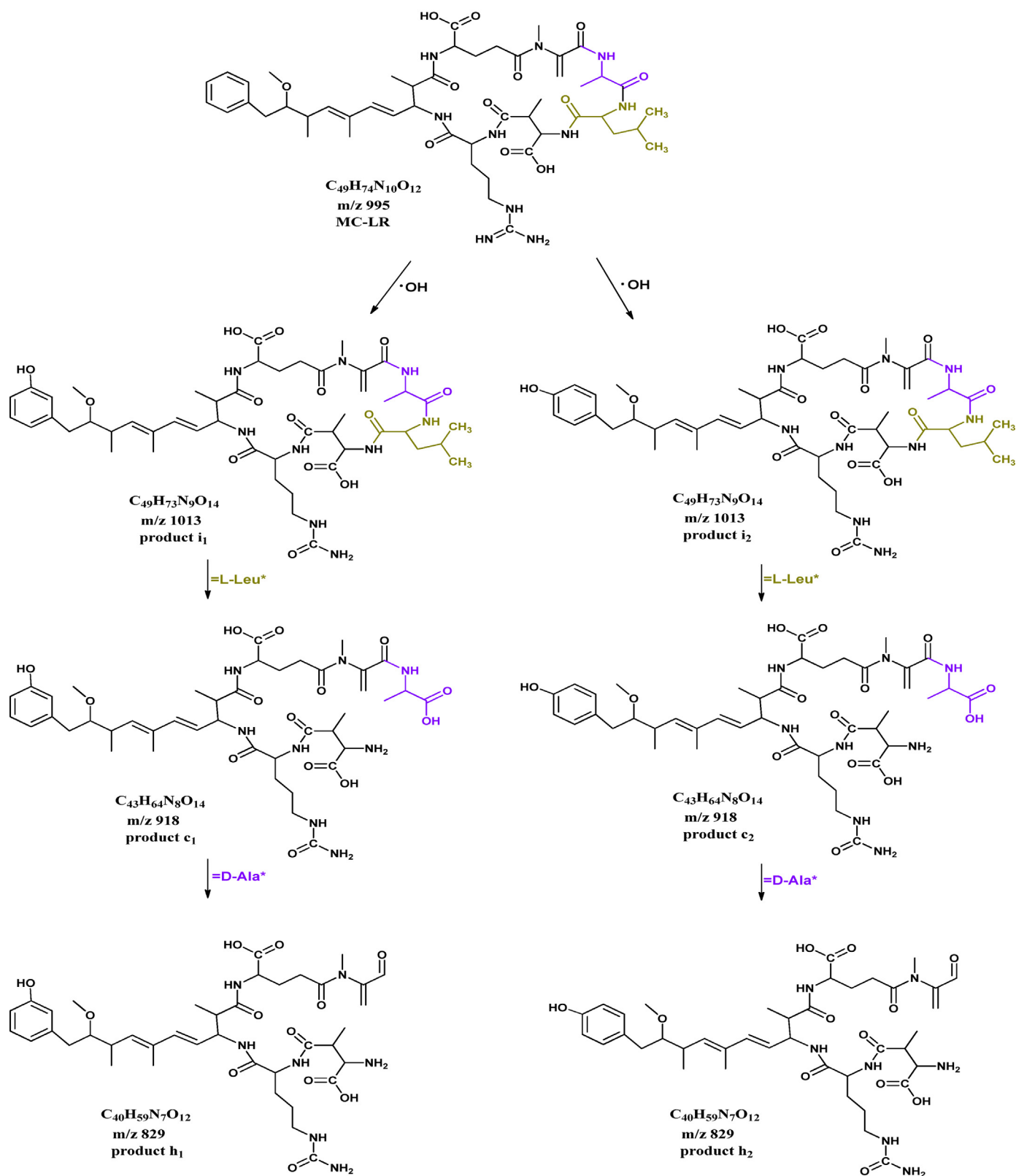
The primary decomposition reaction could be either the catalytic hydrolysis of peptide bonds or the catalytic oxidation of the unsaturated bonds of MC-LR. The primary decomposition route of MC-LR was determined by comparing TOC removal under various reaction conditions since hydrolysis of MC-LR peptide bonds alone would not lead to a change in TOC. Results are shown in Fig. 4 and the general trend is consistent with the data from HPLC analysis of intermediates (see Table 1). There was little change in TOC in the presence of maghemite alone (a) for 25 h. The other two controls, (b) and (c), produced similar (~15%) reductions in TOC resulting

from the degradation (~25%) of MC-LR. This indicates that  $\text{H}_2\text{O}_2$  decomposes to produce  $\cdot\text{OH}$  with and without irradiation. The  $\cdot\text{OH}$  induces degradation similar to that of the Fenton reaction and oxidizes most organic compounds to  $\text{CO}_2$  and  $\text{H}_2\text{O}$ . However, this TOC reduction under visible light irradiation (Fig. 4d) was significantly enhanced (up to 58% TOC removal after 25 h), approaching 100%  $\text{H}_2\text{O}_2$  utilization efficiency, based on Eq. (1).



The maghemite catalyst significantly improves the efficiency of  $\text{H}_2\text{O}_2$  utilization, even in the presence of methanol (~1.6 M, about  $10^6$  times the concentration of MC-LR). To gain insight on





b. Catalytic hydrolysis of MC-LR peptide bonds after hydroxylation of the Adda benzene ring

Fig. 7. (Continued).

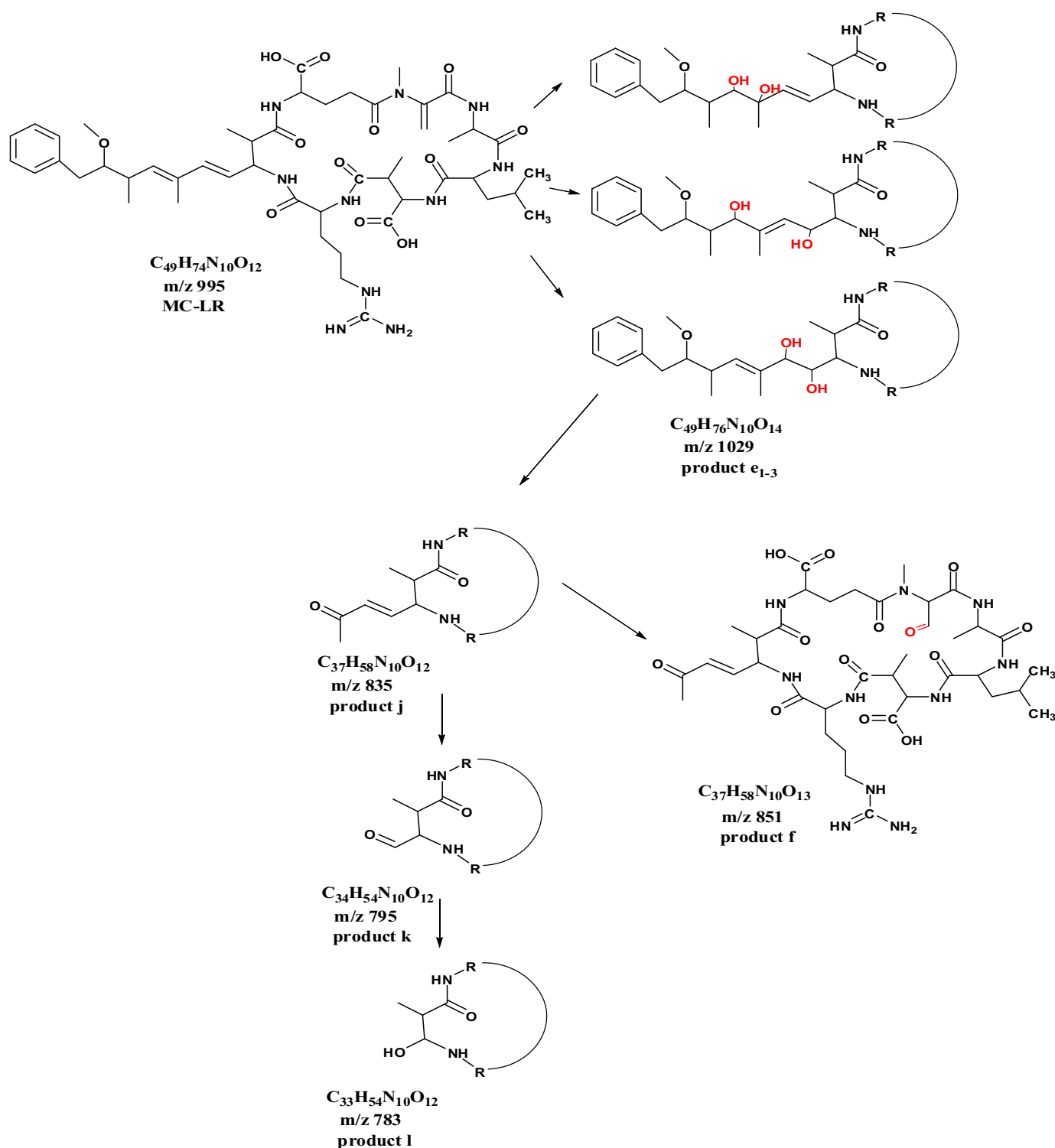


Fig. 8. Intermediates that belong to traditional oxidative pathways for MC-LR degradation by the maghemite system.

the decomposition of MC-LR, the position of the hydrolyzed MC-LR peptide bonds were determined by examining the decomposition intermediates with LC–MS.

The effect of co-existing natural organic matter (NOM) on the degradation efficiency was investigated. Fulvic acid (FA) was used to represent the NOM present in practical treatments [32] and added to the maghemite photocatalytic system used to degrade

MCLR. As shown in Fig. 5, a low concentration of FA ( $c_{FA}/c_{MC-LR} < 10$ ) has a negligible effect on the degradation of MC-LR. Even when the FA concentration was enhanced to 50 times of that of MC-LR, the removal efficiency was 47.9%. These results show that the proposed degradation system is effective in the presence of coexisting NOM, an important practical consideration for treatment of natural waters (Fig. 5).

### 3.2. Identification of intermediates by LC–MS

After a reaction time of 5 h at least twelve intermediate products could be identified in the total ion chromatogram (TIC), shown in Fig. 6. That every of them changes with different reaction times is further observed by TIC in details and summarized in Table 1. In Table 1, the elution times, mass to charge ratios ( $m/z$ ), and peak intensities at various irradiation times are shown for the 12 intermediates and substrate MC-LR. Among all 12 detected intermediates, six resulted from hydrolysis of peptide bonds ( $a$ – $d$ ,  $g$  and  $h$ ), while the other six are typical PCO products ( $e$ ,  $f$  and  $i$ – $l$ ). The hydrolysis products were rarely reported in the literatures on PCO decomposition of MC-LR in water.

The hydrolysis of MC-LR peptide bonds is rapid and loss of a D-MeAsp fragment produces intermediate product  $d$  ( $m/z$  884). Product  $b$  ( $m/z$  700) is then formed by hydrolytic cleavage of the peptide bond connecting Mhda and D-Ala. Products  $a$  ( $m/z$  743) and  $g$  ( $m/z$  759), the primary hydrolysis products, are remnants containing D-Glu and Mdha (see Fig. 7a). With products  $d$  and  $b$ , no oxidation of MC-LR occurs. The conjugated diene in Adda readily undergoes oxidative hydroxylation, but remains intact in products  $a$ ,  $b$ ,  $d$  and  $g$ ; the photocatalytic system preferentially hydrolyses peptide bonds. In the minor products  $d$  and  $g$ , the guanidyl groups on L-Arg is converted to a terminal amine group, consistent with PCO decomposition of the Adda segment [12]. However, they are minor components in the TIC of LC–MS and are formed even in the dark.

Product  $i_{1-2}$  ( $m/z$  1013), with two isomers, contains the hydroxylated phenyl ring of Adda (Fig. 6b). Product  $c_{1-2}$  ( $m/z$  918; only one of the two possible isomers was detected) and  $h_{1-2}$  ( $m/z$  829) result from successive catalytic hydrolysis of the peptide bonds connecting D-MeAsp to L-leu and Mdha to D-Ala (Fig. 7b).

The peak for product  $b$  ( $m/z$  700), rising from the base line to a maximum and then returning to the baseline (Table 1), indicates the cyclic structure of MC-LR was cleaved by catalytic hydrolysis.

The common oxidation products in a PCO process, such as products  $e$ ,  $j$ – $l$ ,  $f$  ( $m/z$  1029, 835, 795, 783, 851), were also detected without concomitant hydrolysis of peptide bonds (Fig. 8).

It is well known that species  $e$  ( $m/z$  1029) is formed by dihydroxylation of the unsaturated bonds of Adda by  $\bullet\text{OH}$  attack, forming the 1, 2 and 1, 4 isomers (see right side of Fig. 8) [33]. However, in the system under investigation, dihydroxylation is not important for MC-LR degradation (see Fig. 6 and Table 1). Product  $f$  ( $m/z$  851) is an oxidation product formed, not by hydrolysis of peptide bonds, but by carbonylation of the methyl group on Meha of product  $j$  ( $m/z$  835) as shown in Fig. 8. Most of the oxidation products, such as product  $a$ – $d$ ,  $g$  and  $h$ , were not similar to those produced by typical PCO, so the present system must involve alternate degradation pathways. Intermediate product fragments that do not occur in a  $\bullet\text{OH}$  dominated process of MC-LR degradation can help explain the key role of catalytic hydrolysis in efficient use of  $\text{H}_2\text{O}_2$  and visible light irradiation.

The last four products  $a$ ,  $c$ ,  $d$  and  $g$  ( $m/z$  743, 918, 884, 759, respectively), produced by hydrolysis of peptide bonds in the MC-LR ring (see the last line of Table 1) are more difficult to eliminate than MC-LR itself. This indicates that the catalyst preferentially interacts with the intact cycle structure of MC-LR, composed of seven amino acids linked by peptide bonds (Fig. 1). After the macrocycle is opened even by a single hydrolysis, the maghemite catalyst has little ability to promote further decomposition. Opening the cycle detoxifies MC-LR, the toxicity of MC-LR was significantly decreased in the photocatalytic degradation process in the toxicity testing (see Fig. S1). Therefore, the selectivity of the maghemite catalyst toward the cyclic structure makes this catalytic system particularly promising.

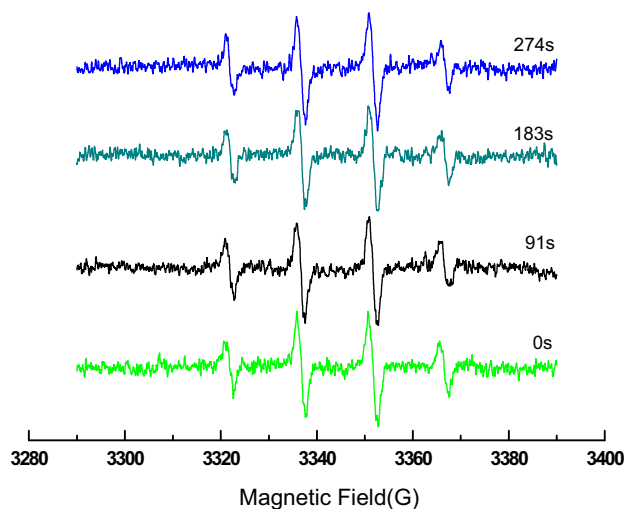
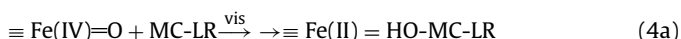
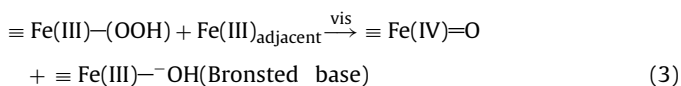
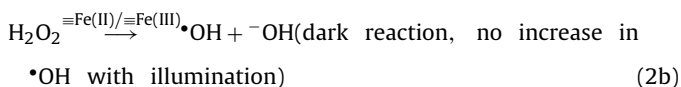
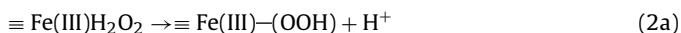


Fig. 9. ESR spectral changes of DMPO- $\bullet\text{OH}$  adducts with time of irradiation. Maghemite powder: 240 mg/L; [DMPO] = 1.3 mol/L; [ $\text{H}_2\text{O}_2$ ] =  $1 \times 10^{-4}$  mol/L; [MC-LR] = 2.0 mg/L.

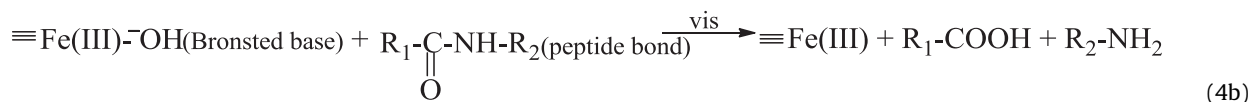
### 3.3. Proposed degradation pathway

To clarify the role of visible light irradiation in the present maghemite photocatalytic system, either accelerating  $\text{H}_2\text{O}_2$  split into  $\bullet\text{OH}$  or other catalytic reaction, ESR with spin-trapping (DMPO) was used to observe the production and change of  $\bullet\text{OH}$  free-radical during both the dark reaction and visible light catalytic reaction (Fig. 9). The DMPO- $\bullet\text{OH}$  adduct signature is a signal with intensity ratio 1:2:2:1 and its presence is a clear indication that  $\bullet\text{OH}$  forms in the dark. Visible light irradiation did little to increase signal intensity, indicating that excitation by visible light does not enhance the formation of  $\bullet\text{OH}$ . This is highly consistent with the findings of Kwan and Voelker [34]; Given that the significantly enhanced MC-LR degradation (Figs. 3 and 4c vs d) caused by visible light irradiation, now it was very distinct that  $\bullet\text{OH}$  free-radical formed on the maghemite surface is not the chief contributions to degradation of MC-LR in the present photocatalytic system.

Based on ESR observations of  $\bullet\text{OH}$  and the fact that catalytically hydrolyzed products dominate in MC-LR decomposition by LC–MS, it is postulated that  $\text{H}_2\text{O}_2$  interacts with the maghemite surface, which is then activated by visible light to produce transient Brønsted base sites and high valence iron (Eq. (3)). Brønsted base sites and the  $\text{Fe(IV)=O}$  species on the maghemite surface then hydrolyze the peptide bonds and oxidize MC-LR (Eq. (4)). This mechanism would not produce more  $\bullet\text{OH}$  under visible light irradiation because the  $\text{H}_2\text{O}_2$  decomposition, catalyzed by  $\text{Fe(II)/Fe(III)}$  (Eq. (2b)), proceeds very rapidly, even in the dark. Visible light plays a crucial role in the formation of Brønsted base sites (Eq. (3)) and regeneration of active ferric sites (Eq. (4b)).







Note:  $\equiv\text{Fe(III)}$  represents active ferric sites on the maghemite surface, to which  $\text{H}_2\text{O}$  adsorbs or coordinates prior to catalytic action.

To completely elucidate this possible mechanism, more direct evidence will be necessary; for example, in situ analysis of  $\text{Fe(III)}/\text{Fe(II)}$  transformation by XPS and FTIR spectroscopy. We are working fast to approach to this mechanism.

#### 4. Conclusions

Maghemite was employed as a photocatalyst to decompose MC-LR in water. Based on  $\text{H}_2\text{O}_2$  consumption, both MC-LR transformation and TOC removal occurred at near 100% efficiency. The production of  $\cdot\text{OH}$  in the dark was the same as under visible light, very atypical of PCO systems. Twelve intermediate products were identified by LC-MS and half originated from catalytic hydrolysis of the peptide bonds of MC-LR. Based on these results, we postulate that  $\text{H}_2\text{O}_2$  is used to generate both high valence iron ( $\text{Fe(IV)=O}$ ) and the Brønsted base,  $\text{Fe(III)}-\text{OH}$ , via a MLCT process. The catalytic system selectively detoxifies MC-LR by predominantly hydrolyzing the peptide bonds of the ring structure. Because the maghemite catalyst targets peptide bonds, detoxification of MC-LR in the presence of NOM appears feasible.

#### Acknowledgments

This work was funded by the National Natural Science Foundation of China (Nos. 21377067, 21207079 and 21177072), Natural Science Foundation for Innovation Group of Hubei Province, China (No. 2009CDA020) and Hubei Provincial Department of Education Science Research Project Youth Talent Project (Q20141208). We also would like to thank Dr. Zhao Bo of Department of Pharmacology, Medical Science College (CTGU, China) for his assistance in Toxicity Testing.

#### Appendix A. Supplementary data

Supplementary data associated with this article can be found, in the online version, at <http://dx.doi.org/10.1016/j.apcatb.2014.05.016>.

#### References

- [1] W.W. Carmichael, *Sci. Am.* 270 (1994) 64–70.
- [2] J. Mankiewicz, M. Tarczynska, Z. Walter, M. Zalewski, *Acta Biol. Crac. Ser. Bot.* 45 (2003) 9–20.
- [3] T. Krishnamurthy, W.W. Carmichael, E.W. Sarver, *Toxicon* 24 (1986) 865–873.
- [4] C.F.B. Holmes, J.T. Maynes, K.R. Perreault, J.F. Dawson, M.N.G. James, *Curr. Med. Chem.* 9 (2002) 1981–1989.
- [5] R.M. Dawson, *Toxicon* 36 (1998) 953–962.
- [6] M.M. Gehringer, *FEBS Lett.* 557 (2004) 1–8.
- [7] S. Imanishi, K. Harada, *Toxicon* 43 (2004) 651–659.
- [8] E. Alverca, M. Andrade, E. Dias, B.F. Sam, M.C.C. Batoreu, P. Jordan, M.J. Silva, P. Pereira, *Toxicon* 54 (2009) 283–294.
- [9] J. Dunn, *Br. Med. J.* 312 (1996) 1183–1184.
- [10] WHO (World Health Organization), *Guide Lines for Drinking Water Quality*, 3rd ed., World Health Organization, Geneva, 2004.
- [11] M.G. Antoniou, J.A. Shoemaker, A.A. De la Cruz, P.A. Nicolaou, D.D. Dionysiou, *Appl. Catal. B: Environ.* 91 (2009) 165–173.
- [12] Y. Fang, Y. Huang, J. Yang, P. Wang, G. Cheng, *Environ. Sci. Technol.* 45 (2011) 1593–1600.
- [13] A.J. Feitz, T.D. Waite, *Environ. Sci. Technol.* 37 (2003) 561–568.
- [14] M.G. Antoniou, J.A. Shoemaker, A.A. de la Cruz, D.D. Dionysiou, *Toxicon* 51 (2008) 1103–1118.
- [15] Y. Zhong, X. Jin, R. Qiao, X.H. Qi, Y.Y. Zhang, *J. Hazard. Mater.* 167 (2009) 1114–1118.
- [16] K. Hanna, T. Kone, G. Medjahdi, *Catal. Commun.* 9 (2008) 955–959.
- [17] G.B. Ortiz de la Plata, O.M. Alfano, A.E. Cassano, *Chem. Eng. J.* 137 (2008) 396–410.
- [18] G. Smith, *Can. Mineral.* 15 (1977) 500–507.
- [19] S.S. Lin, M.D. Gurol, *Environ. Sci. Technol.* 32 (1998) 1417–1423.
- [20] M.L. Estapa, E. Boss, L.M. Mayer, C.S. Roesler, *Limnol. Oceanogr.* 57 (2012) 97–112.
- [21] D.G. Bourne, G.J. Jones, R.L. Blakeley, A. Jones, A.P. Negri, P. Riddles, *Appl. Environ. Microbiol.* 62 (1996) 4086–4094.
- [22] C. Motti, R. Quinn, P. Alewood, *Bioorg. Med. Chem. Lett.* 6 (1996) 2107–2112.
- [23] L. Lawrence, W.J. Moore, *J. Am. Chem. Soc.* 73 (1951) 3973–3977.
- [24] D. Kahne, W.C. Still, *J. Am. Chem. Soc.* 110 (1988) 7529–7534.
- [25] E.L. Hogg, J.N. Burstyn, *J. Am. Chem. Soc.* 117 (1995) 7015–7016.
- [26] P.H. Ho, K. Stroobants, T.N. Parac-Vogt, *Inorg. Chem.* 50 (2011) 12025–12033.
- [27] G. Absillis, T.N. Parac-Vogt, *Inorg. Chem.* 51 (2012) 9902–9910.
- [28] K. Marshall-Bowman, S. Ohara, D.A. Sverjensky, R.M. Hazen, H.J. Cleaves, *Geochim. Cosmochim. Acta* 74 (2010) 5852–5861.
- [29] E. Schreiner, N.N. Nair, C. Wittekindt, D. Marx, *J. Am. Chem. Soc.* 133 (2011) 8216–8226.
- [30] R.J. Watts, J. Sarasa, F.J. Loge, A.L. Teel, *J. Environ. Eng.* 131 (2005) 158–164.
- [31] J.K. Fawell, R.E. Mitchell, D.J. Everett, R.E. Hill, *Hum. Exp. Toxicol.* 18 (1999) 162–167.
- [32] P. Sharma, M. Rolle, B. Kocar, S. Fendorf, A. Kappler, *Environ. Sci. Technol.* 45 (2011) 546–553.
- [33] Y.F. Fang, W.H. Ma, Y.P. Huang, G.W. Cheng, *Chem. Eur. J.* 19 (2013) 3224–3229.
- [34] W.P. Kwan, B.M. Voelker, *Environ. Sci. Technol.* 37 (2003) 1150–1158.